

# PCCP

Accepted Manuscript



This is an *Accepted Manuscript*, which has been through the Royal Society of Chemistry peer review process and has been accepted for publication.

*Accepted Manuscripts* are published online shortly after acceptance, before technical editing, formatting and proof reading. Using this free service, authors can make their results available to the community, in citable form, before we publish the edited article. We will replace this *Accepted Manuscript* with the edited and formatted *Advance Article* as soon as it is available.

You can find more information about *Accepted Manuscripts* in the [Information for Authors](#).

Please note that technical editing may introduce minor changes to the text and/or graphics, which may alter content. The journal's standard [Terms & Conditions](#) and the [Ethical guidelines](#) still apply. In no event shall the Royal Society of Chemistry be held responsible for any errors or omissions in this *Accepted Manuscript* or any consequences arising from the use of any information it contains.

**Fano resonance in a gold nanosphere with a J-aggregate coating**

Andrew M. Fales<sup>1,2</sup>, Stephen J. Norton<sup>1,2</sup>, Bridget M. Crawford<sup>1,2</sup>, Brendan G. DeLacy<sup>4</sup>, Tuan Vo-Dinh<sup>1,2,3</sup> (\*)

<sup>1</sup> Fitzpatrick Institute for Photonics, Duke University, Durham, NC, 27708, USA

<sup>2</sup> Department of Biomedical Engineering, Duke University, Durham, NC, 27708, USA

<sup>3</sup> Department of Chemistry, Duke University, Durham, NC, 27708, USA

<sup>4</sup> U.S. Army Edgewood Chemical Biological Center, Aberdeen Proving Ground, Maryland 21010, USA

(\*) Corresponding Author: tuan.vodinh@duke.edu

**Abstract**

We present a facile method to induce J-aggregate formation on gold nanospheres in colloidal solution using polyvinylsulfate. The nanoparticle J-aggregate complex results in an absorption spectrum with a split lineshape due to plasmon-exciton coupling, i.e. via the formation of upper and lower plexcitonic branches. The use of nanoparticles with different plasmon resonances alters the position of the upper plexcitonic band while the lower band remains at the same wavelength. This splitting is investigated theoretically, and shown analytically to arise from Fano resonance between the plasmon of the gold nanoparticles and exciton of the J-aggregates. A theoretical simulation of a J-aggregate coated and uncoated gold nanosphere produces an absorption spectrum that shows good agreement with the experimentally measured spectra.

**1. Introduction**

Coupling of the exciton resonance of a J-aggregate coating with the localized surface plasmon resonance (LSPR) of the metallic core of a plasmonic nanoparticle gives rise to an asymmetric resonance exhibiting the characteristic Fano lineshape. Fano resonances generated by composite nanostructures have been proposed for biomolecular sensing because of the sensitivity of the Fano phenomenon to the local environment.<sup>1</sup> There are various hybrid systems coupling plasmon and exciton resonances to generate hybridized energy states, referred to as plexcitons, for a wide variety of applications, ranging from chemical sensing to bioenergy-

related research.<sup>2-12</sup> These hybridized energy states are manifested in the formation of a blue-shifted peak (upper plexcitonic branch), and a red-shifted peak (lower plexcitonic branch). Here we report absorption measurements of a J-aggregate compound coating a gold nanosphere that displays the characteristics of Fano interference. The Fano lineshape can be described as a consequence of the coupling between a sharp resonance, in this case the J-aggregate response, and a broader resonance, here provided by the plasmon response.<sup>13,14</sup> This coupling between the two modes produces a partial “quenching” of the plasmon response by the J-aggregate resonance, or equivalently, an induced-transparency in the absorption cross section of the particle.<sup>15</sup> Evidence of the latter is a “Fano dip” in the extinction spectrum near the J-aggregate resonance. Recent reports have theoretically shown Fano resonances in spherical and cylindrical core-shell scatterers.<sup>16,17</sup> While Arruda *et. al.* presented a similar analysis to the one performed in this study, one key difference is that they consider a plasmonic core with a dielectric coating, while we consider a plasmonic core with a J-aggregate layer. As shown below, the spherical symmetry of the metallic core with the J-aggregate layer is sufficiently simple to show analytically that their interaction produces the classic Fano lineshape. Letting  $\omega_b$  and  $\omega_s$  denote, respectively, the broad and sharp resonances and  $\gamma_b$  and  $\gamma_s$  their corresponding line widths, this Fano response takes the form

$$F(\omega) = \frac{(\kappa + q)^2}{\kappa^2 + 1}, \quad (1)$$

where  $\kappa = (\omega^2 - \omega_s^2 - \omega_s \Delta) / \Gamma$ ,  $q = (\omega_s^2 - \omega_b^2) / \gamma_b \omega_s$ ,  $\Delta = (\omega_s^2 - \omega_b^2) / \omega_s$  and  $\Gamma = \gamma_s \omega_s$ .<sup>18</sup> Here we have assumed that  $\gamma_s \ll \gamma_b$ . We show in a later section that the response of the J-aggregate on the gold particle can be placed in the form of (1) thus confirming the experimental results with theoretical studies.

## 2. Experimental

### Materials

All chemicals were purchased from Sigma-Aldrich (St. Louis, MO, USA) at the highest purity available unless otherwise specified. Ultrapure water (18 M $\Omega$ •cm) was used in all preparations. Glassware and stir bars were cleaned with *aqua regia* before use. Gold nanorods with peak

plasmon wavelengths at 550 nm, 600 nm, 650 nm, and 750 nm were purchased from Nanopartz Inc. (Loveland, CO, USA).

### **Instrumentation**

UV/Vis spectra were recorded on a FLUOstar Omega plate reader (BMG LABTECH GmbH, Germany). TEM micrographs were acquired on a FEI Tecnai G<sup>2</sup> Twin transmission electron microscope (Hillsboro, OR, USA).

### **Nanoparticle synthesis (AuNP)**

The gold nanospheres were synthesized using a modified Turkevich method. A 100 mL solution of 0.25mM HAuCl<sub>4</sub> was brought to a rolling boil under vigorous stirring. The reduction process was initiated by injecting 0.7 mL of 1% citrate solution. The solution immediately turned clear, followed by a slow transition to dark grey and then deep red. After this point, the solution was kept boiling for another 30 minutes, maintaining the initial volume, before being cooled to room temperature. This resulted in particles with a plasmon peak at 540 nm. The nanoparticles with plasmons at 532 and 520 nm were produced by altering the amount of citrate added to 1 mL and 2 mL, respectively.

### **PIC sample preparation**

A 0.5mM stock solution of 1,1-Diethyl-2,2-cyanine iodide (PIC) was prepared in 0.1M phosphate buffer, pH 6.0. PIC J-aggregate formation was induced by diluting the stock solution into 5M NaCl; when diluted into water, no J-aggregate formation is observed. For J-aggregate formation on the gold nanoparticles or nanorods, the particles were first coated with a polymer, poly(vinylsulfonic acid, sodium salt) solution (PVSA), at 0.02% w/v to stabilize them against aggregation. The PIC stock solution could then be added at the desired concentration to the PVSA-coated gold nanospheres or nanorods (AuNP-PVSA or AuNR-PVSA).

## **3. Results and Discussion**

The formation of J-aggregates by PIC has been well documented in the literature.<sup>2-11</sup> A simple method to induce J-aggregate formation is by increasing the salt concentration of the dye solution. As shown in Figure 1, when the PIC stock solution is diluted into water, no J-

aggregates are observed. When 5M NaCl is used in place of water, the J-aggregate peak can be seen at 575 nm. The interaction of these J-aggregates with gold nanoparticles was studied by adding aliquots of the PIC stock solution to PVSA-coated gold nanoparticles.

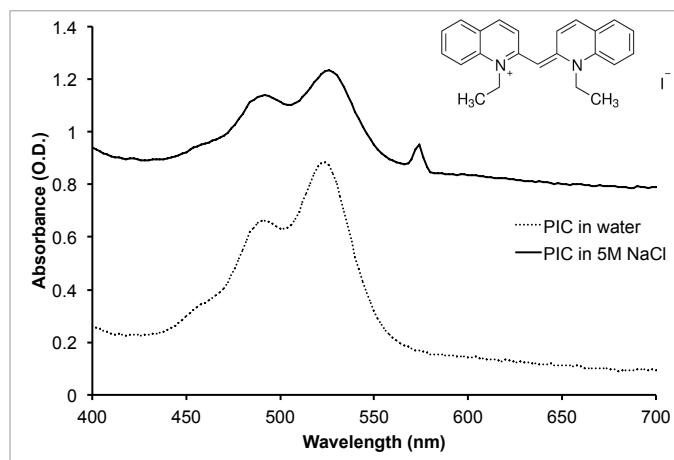


**Figure 1.** UV/Vis absorption spectra of 20 $\mu$ M PIC in water (dotted) and in 5M NaCl (solid). The new peak observed at about 575 nm indicates the presence of J-aggregates in the solution. The chemical structure of PIC is shown at the top right.

The PVSA was used to serve two purposes in this study. First, the gold nanoparticles were protected against aggregation in the presence of PIC. Without the polymer coating, the color of the nanoparticle solution changed immediately upon addition of PIC and the particles began to settle out of solution. Second, the negatively charged PVSA aided in electrostatic interaction with the positively charged PIC. To determine the optimal amount of PIC for interaction with the gold nanoparticles, a range of PIC concentrations were added to AuNP-PVSA before UV/Vis spectra were recorded. Figure 2 shows the extinction spectra of the AuNP-PVSA and PIC complexes. As shown, the magnitude of the induced transparency at around 580 nm levels off after the concentration of PIC reaches 20 $\mu$ M. This concentration was then selected for further investigation.

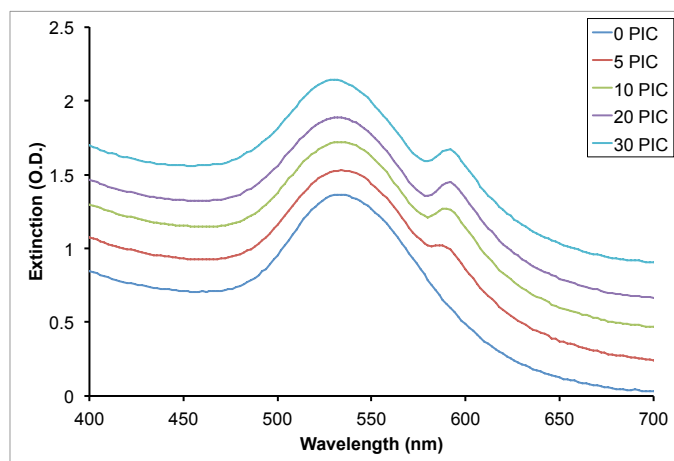


**Figure 2.** UV/Vis spectra of AuNP-PVSA with different concentrations (in  $\mu\text{M}$ ) of PIC. The spectra have been offset for clarity.

Three different sizes of nanoparticles were prepared to see what effect, if any, this would have on the Fano lineshape. By keeping the concentration of gold constant and varying the amount of citrate, gold nanoparticles with a plasmon resonance of 520 nm, 532 nm, and 540 nm were produced (Figure 3A). This corresponds to nanoparticle sizes of approximately 15 nm, 40 nm, and 60 nm, respectively (Figure 3(C-E)). All three sizes of nanoparticles were shown to produce the Fano lineshape after forming a complex with PIC, consisting of a spectral dip at about 580 nm and a new peak at approximately 593 nm (Figure 3B). The original surface plasmon resonance wavelength of the sample is retained as the upper band in the split lineshape.

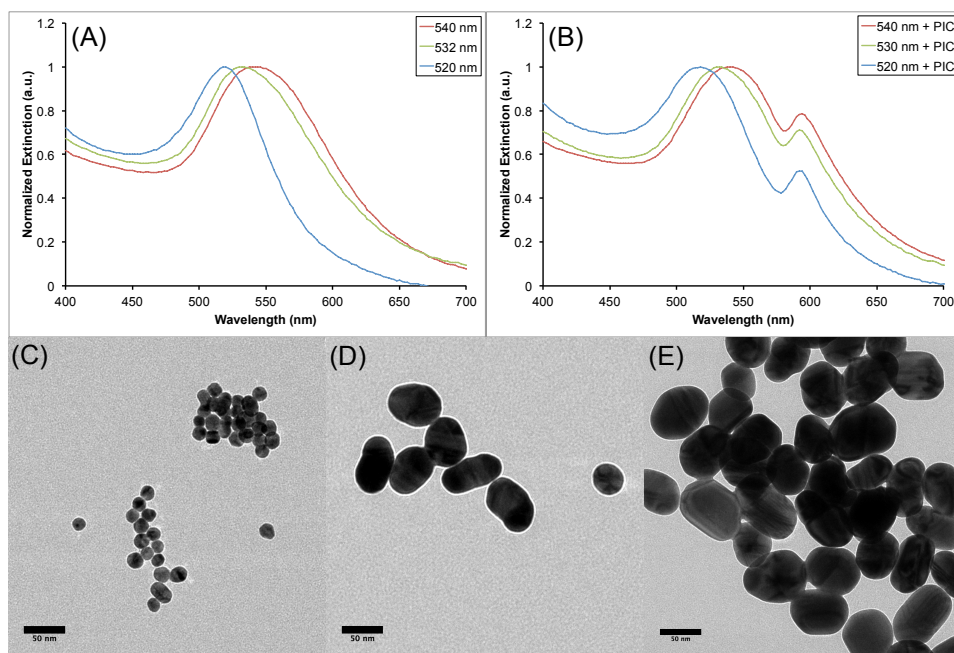


**Figure 3.** (A) Normalized extinction spectra of the three different nanosphere samples, labeled by their peak plasmon resonance. (B) Normalized extinction spectra of the nanosphere + 20  $\mu$ M PIC samples. (C-E) TEM images of the 520 nm, 532 nm, and 540 nm samples, respectively. Scale bars are 50 nm.

The unnormalized extinction spectra of the AuNP-PVSA and AuNP-PVSA + PIC complexes are shown in Figure 4. After addition of PIC, there is a decrease in the extinction maxima at the plasmon resonance wavelength, accompanied by an increase in extinction at 593 nm, with a dip between the two peaks occurring at 580 nm. In all three cases, the lower band remains at 593 nm, while the upper band position is dependent on the initial surface plasmon resonance wavelength of the nanoparticles. Thus, the 520 nm plasmon particles have the largest gap between the upper and lower plexcitonic branches at 73 nm, and the 540 nm plasmon particles have the smallest gap at 53 nm.

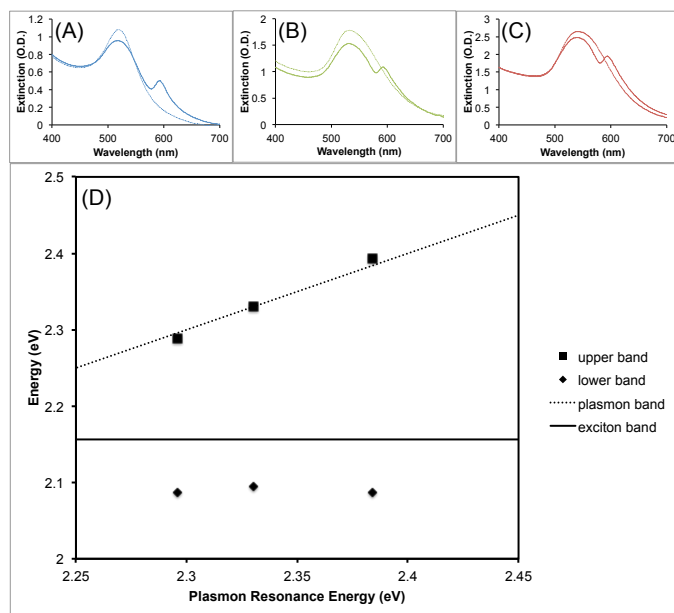


**Figure 4.** Extinction spectra of the AuNP-PVSA (dotted) and AuNP-PVSA + PIC complex (solid) for the 520 nm (A), 532 nm (B), and 540 nm (C) plasmon samples. (D) Energy diagram of the upper and lower plexcitonic branches for the three different nanoparticle samples, extracted from the aforementioned spectra.

To better visualize the splitting between the upper and lower plexcitonic branches, an energy diagram was created (Figure 4D). As we have already observed, the upper band of the split lineshape closely follows the initial surface plasmon resonance of the nanoparticles, while the lower band is essentially unchanged between the three samples. This phenomenon results from coherent coupling between the exciton and plasmon dipoles, producing a constructive interference that leads to the increase in extinction at 593 nm.<sup>2</sup> The energy difference between the upper and lower bands for the 520 nm, 532 nm, and 540 nm plasmon nanoparticles was determined to be 306 meV, 236 meV, and 200 meV, respectively; these values are in line with those reported in previous works.<sup>5,11,19-21</sup> Because the gold nanosphere plasmon cannot be tuned to cross the exciton band, it is unknown whether the lower band will remain constant or display the expected anti-crossing behavior of hybridized plexcitons. For further investigation, we have used gold nanorods with plasmons on both sides of the exciton peak to more fully understand the induced Fano lineshape.



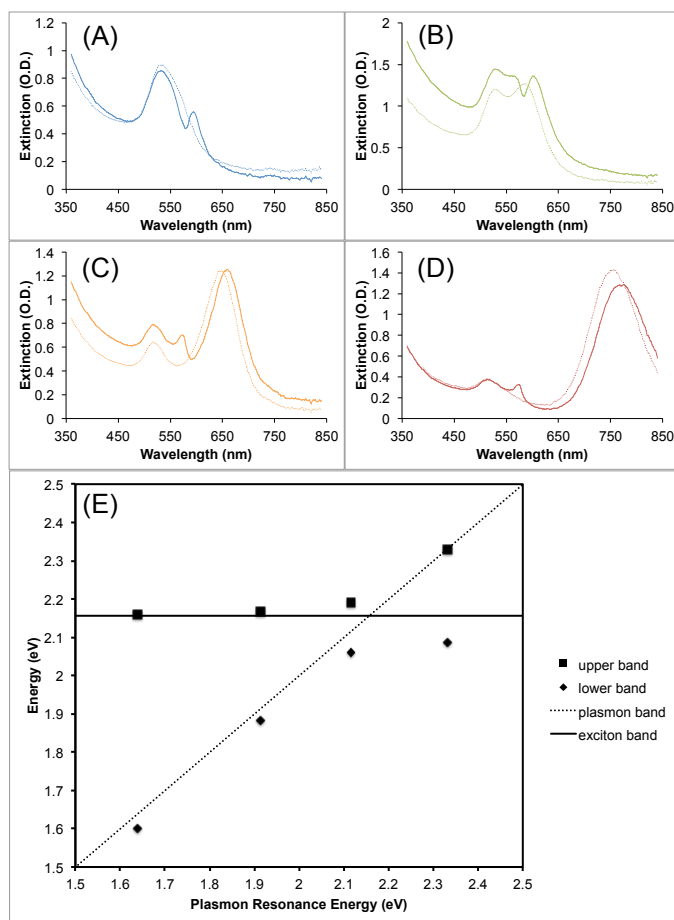


**Figure 5.** Extinction spectra of the AuNR-PVSA (dotted) and AuNR-PVSA + PIC complex (solid) for the 550 nm (A), 600 nm (B), 650 nm (C), and 750 nm (D) plasmon samples. (E) Energy diagram of the upper and lower plexcitonic branches for the four different nanorod samples, extracted from the aforementioned spectra.

The gold nanorods used in this experiment had a residual coating of cetyltrimethylammonium bromide (CTAB) prior to PVSA functionalization. It is possible that the PVSA does not displace the CTAB bilayer, leaving a  $\sim 6$  nm gap between the nanorod surface and PVSA layer. This would reduce the coupling between the nanorod plasmon and J-aggregate exciton, resulting in a shallower “Fano dip” in the extinction spectra. Complete removal of the CTAB layer may provide stronger plexcitonic coupling, however, further investigation of this topic is beyond the scope of this manuscript. Figure 5(A-D) shows the extinction spectra of the four different nanorod samples before (dotted) and after (solid) PIC coating. The nanorod samples had longitudinal plasmon resonances of 550 nm, 600 nm, 650 nm, and 750 nm, spanning across both sides of the J-aggregate exciton band. As shown in Figure 5E, the typical anti-crossing behavior

is observed as the gold nanorod longitudinal plasmon resonance is tuned across the J-aggregate exciton peak, confirming strong coupling between the nanoparticle plasmon and J-aggregate exciton. The further the nanorod plasmon resonance is from the J-aggregate absorption, the larger the energy difference between the split peaks; a similar trend was observed for the nanospheres in Figure 4. These results suggest that if the gold nanosphere plasmon could be tuned to cross the exciton wavelength, anti-crossing of the upper and lower plexcitonic branches would also be observed.

#### 4. Theoretical Analysis

We show in this section that the coupling between the plasmonic resonance of the gold core and the J-aggregate layer gives rise to a Fano resonance that can be expressed in the standard Fano form. Denote the layer and core dielectric constants by  $\epsilon_j$  and  $\epsilon_{au}$ , respectively, and the background dielectric constant by  $\epsilon_m$ . We model the response of the J-aggregate compound using a Lorentzian lineshape of the form

$$\epsilon_j(\omega) = \epsilon_{j\infty} + \frac{f\omega_0^2}{\omega_0^2 - \omega^2 - i\omega\gamma_j}, \quad (2)$$

where  $\omega_0$  is the primary J-aggregate transition line,  $f$  is the oscillator strength and  $\gamma_j$  is the resonance linewidth. We employ a simple Drude model for the dielectric constant of the gold core:

$$\epsilon_{au}(\omega) = \epsilon_\infty - \frac{\omega_p^2}{\omega^2 + i\omega\gamma_{au}}, \quad (3)$$

where  $\omega_p$  is the plasmon frequency for gold and  $\gamma_{au}$  is the plasmon linewidth. Let  $R$  and  $R_c$  denote respectively the radius of the coated particle and the radius of the gold core. The layer thickness is then  $t = R - R_c$ , where we assume the thickness is much smaller than the particle radius ( $t \ll R$ ). We also assume that the particle is much smaller than the optical wavelength so that the quasistatic approximation can be employed. The polarizability of the particle is then given by

$$\alpha = 3V \left[ \frac{(\epsilon_j - \epsilon_m)(2\epsilon_j + \epsilon_{au}) + (2\epsilon_j + \epsilon_m)(\epsilon_{au} - \epsilon_j)(R_c / R)^3}{(\epsilon_j + 2\epsilon_m)(2\epsilon_j + \epsilon_{au}) + 2(\epsilon_j - \epsilon_m)(\epsilon_{au} - \epsilon_j)(R_c / R)^3} \right], \quad (4)$$

where  $V$  is the particle volume. The scattering and absorption cross sections are

$$\sigma_s = \frac{k^4}{6\pi} |\alpha|^2 \quad (5)$$

$$\sigma_a = k \operatorname{Im}\{\alpha\}, \quad (6)$$

where  $k$  is the wavenumber in the host medium. We can simplify (4) under the assumption of a thin layer. Expanding  $(R_c/R)^3$  to first order in the thickness  $t$  by writing

$(R_c/R)^3 = (1-t/R)^3 \approx 1-3t/R$  and substituting into (4) gives

$$\alpha = 3V \left[ \frac{\epsilon_j(\epsilon_{au} - \epsilon_m) - \tau(2\epsilon_j + \epsilon_m)(\epsilon_{au} - \epsilon_j)}{\epsilon_j(\epsilon_{au} + 2\epsilon_m) - 2\tau(\epsilon_j - \epsilon_m)(\epsilon_{au} - \epsilon_j)} \right] \quad (7)$$

where  $\tau \equiv t/R$ .<sup>i</sup>

To show how Fano interference arises in this system, we neglect for simplicity the J-aggregate damping in (2) by setting  $\gamma_j = 0$ . This can usually be justified by noting that

typically  $\gamma_j \ll \gamma_{au}$ . To further simplify the analysis, we shall consider the case in which

$\epsilon_{j\infty} = \epsilon_\infty = \epsilon_m$  in (2) and (3). It is convenient to define  $\tilde{\omega}_0 \equiv \omega_0 \sqrt{1+f/\epsilon_m}$  and  $\tilde{\omega}_{au} \equiv \omega_p / \sqrt{3\epsilon_m}$ ,

where the frequency  $\tilde{\omega}_{au}$  corresponds to the plasmon resonance of the gold core in the absence

of the layer (when  $\tau = 0$ ). Substituting (2) and (3) into (7) and multiplying numerator and

denominator by  $(\omega_0^2 - \omega^2)(\omega^2 + i\omega\gamma_{au})$  results in

$$\alpha = - \left( \frac{V\omega_p^2}{\epsilon_m} \right) \frac{\omega^2 - \tilde{\omega}_0^2 + \tau P}{(\omega^2 - \tilde{\omega}_0^2)(\omega^2 - \tilde{\omega}_{au}^2 + i\omega\gamma_{au}) - \tau Q}, \quad (8)$$

where

$$P \equiv 3(f\omega_0^2/\omega_p^2 - 1)\omega^2 + (3 + 2f/\epsilon_m)\omega_0^2 \quad (9)$$

$$Q \equiv 2f\omega_0^2\tilde{\omega}_{au}^2. \quad (10)$$

<sup>i</sup> This approximation can be avoided for thicker layers by replacing  $\tau$  everywhere by  $\tau - \tau^2 + \tau^3/3$ .

In deriving (9) and (10), we have dropped terms of order  $f^2$ , since typically  $f \ll 1$ , and terms of order  $f\gamma_{au}/\omega$ . The response is quenched for the value of  $\omega = \omega_q$  for which the numerator of (8) vanishes. Setting the numerator to zero, we find that

$$\omega_q^2 = \frac{\tilde{\omega}_0^2 - \tau\omega_0^2(3 + 2f/\epsilon_m)}{1 + 3\tau(f\omega_0^2/\omega_p^2 - 1)}.$$

We note that only partial quenching will occur when the J-aggregate linewidth,  $\gamma_j$ , is nonzero.

The resonances are determined by the zeros of the real part of the denominator of (8), or the solution to

$$(\omega^2 - \tilde{\omega}_{au}^2)(\omega^2 - \tilde{\omega}_0^2) - 2\tau f\omega_0^2\tilde{\omega}_{au}^2 = 0.$$

Assuming that the term proportional to  $\tau f$  is small compared to  $|\tilde{\omega}_{au}^2 - \tilde{\omega}_0^2|$ , the resonant frequencies  $\tilde{\omega}_{au}$  and  $\tilde{\omega}_0$  are shifted slightly. To first order in  $\tau f$  the plasmon resonance  $\tilde{\omega}_{au}$  is shifted to  $\bar{\omega}_{au}$ , given by

$$\bar{\omega}_{au}^2 = \tilde{\omega}_{au}^2 + \frac{2\tau f\omega_0^2\tilde{\omega}_{au}^2}{\tilde{\omega}_{au}^2 - \tilde{\omega}_0^2}.$$

The J-aggregate resonance is also shifted by an amount proportional to  $\tau f$ , which we denote by  $\bar{\omega}_0$ :

$$\bar{\omega}_0^2 = \tilde{\omega}_0^2 - \frac{2\tau f\omega_0^2\tilde{\omega}_{au}^2}{\tilde{\omega}_{au}^2 - \tilde{\omega}_0^2}.$$

To show how Fano behavior is manifested by this system, we follow an approach used by Gallinet and Martin in their analysis of two coupled harmonic oscillators as an illustration of Fano interference in a mechanical system.<sup>22</sup> In our case, the product  $\tau f$  plays the role of the coupling parameter. We begin by expanding the denominator of (8) about the J-aggregate resonance  $\tilde{\omega}_0$ . When  $\omega$  is near  $\tilde{\omega}_0$ , the factor  $\omega^2 - \tilde{\omega}_{au}^2 - i\omega\gamma_{au}$  in the denominator is slowly varying and we replace it with  $C \equiv \tilde{\omega}_0^2 - \tilde{\omega}_{au}^2 - i\tilde{\omega}_0\gamma_{au}$ . On evaluating  $|\alpha|^2$  and  $\text{Im}\{\alpha\}$ , we find that the cross sections become after some manipulation

$$\sigma_s = A \frac{(\kappa + p)^2}{\kappa^2 + 1} \quad (11)$$

$$\sigma_a = B \frac{(\kappa + q)^2 - b}{\kappa^2 + 1}, \quad (12)$$

where

$$\kappa = \frac{1}{\Gamma} \left[ \omega^2 - \tilde{\omega}_0^2 + \frac{\tau Q (\tilde{\omega}_{au}^2 - \tilde{\omega}_0^2)}{|C|^2} \right]$$

$$\Gamma = \frac{\tau Q \tilde{\omega}_0 \gamma_{au}}{|C|^2}$$

$$p = \frac{\tilde{\omega}_0^2 - \tilde{\omega}_{au}^2}{\tilde{\omega}_0 \gamma_{au}} + \frac{P |C|^2}{Q \tilde{\omega}_0 \gamma_{au}}$$

$$q = \frac{\tilde{\omega}_0^2 - \tilde{\omega}_{au}^2}{\tilde{\omega}_0 \gamma_{au}} + \frac{P |C|^2}{2Q \tilde{\omega}_0 \gamma_{au}}$$

and  $A = (k^2 V \omega_p^2 / \epsilon_m |C|)^2 / 6\pi$ ,  $B = -kV \omega_p^2 / \epsilon_m |C|$ ,  $b = (\tau P / 2\Gamma)^2$ . Equation (11) is in the classic Fano form given by (1), but both (11) and (12) display the characteristic asymmetric resonance arising from the ‘‘Fano dip’’ which occurs when  $\kappa + p \approx 0$  in (11) and when  $(\kappa + q)^2 - b \approx 0$  in (12).

## 5. Simulation

Figure 6 shows a calculation of the absorption cross-section using (4) and (12) with the values  $\epsilon_m = 1.77$ ,  $R = 20$  nm,  $R_c = 19$  nm, and in (2)  $\omega_0 = 2\pi c / \lambda_0$  with  $\lambda_0 = 575$  nm,  $\gamma_j = 0.02\omega_0$  and  $f = 0.01$ . For this choice of parameters, one can show that the scattering cross section is insignificant compared to the absorption cross section. The dielectric constant for gold,  $\epsilon_{au}(\omega)$ , was derived from data published in the Handbook of Optical Constants of Solids.<sup>23</sup> The dip in the absorption cross section at about 565 nm corresponds to the ‘‘quenching’’ or induced-transparency of the particle absorption due to the J-aggregate layer. The calculated lineshape closely resembles the experimental spectrum in Figure 4A.

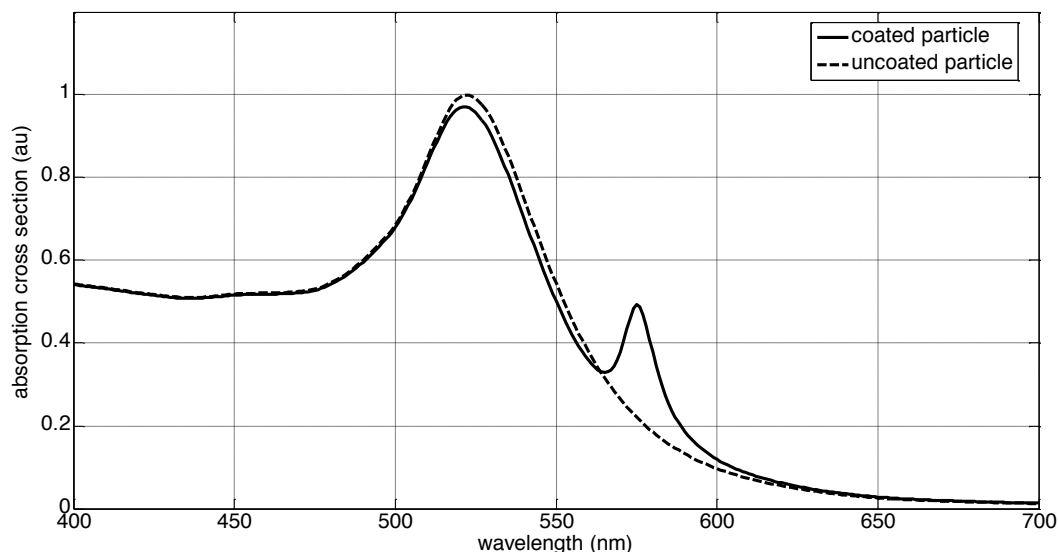


**Figure 6.** Calculation of the absorption cross section with and without the J-aggregate coating.

## 6. Conclusion

Polymer coated gold nanospheres were shown to promote J-aggregate formation of PIC dye on the nanoparticle surface. Coupling between the plasmon of the nanoparticles and exciton of the J-aggregates produced a Fano lineshape, showing an upper and lower plexcitonic band. The size of nanoparticles used affected the position of the upper plexcitonic band, but had no effect on the lower band. The largest splitting energy was found to be 306 meV, for the gold nanoparticles with a plasmon resonance at 520 nm. The observed splitting was shown analytically to be due to Fano resonance between the gold nanoparticle and J-aggregates. Gold nanorods were used to confirm strong coupling between the nanoparticle plasmon and J-aggregate exciton by displaying the typical anti-crossing behavior. A simulated absorption spectrum of a J-aggregate coated gold nanosphere showed good agreement with the experimentally measured spectra.

## Acknowledgements

This work was sponsored by the Duke University Faculty Exploratory Project, the Army Research Office (Grant # W911NF-09-1-0539), and the Department of Energy (Grant # SC0014077).

## References

- (1) Wu, C.; Khanikaev, A. B.; Adato, R.; Arju, N.; Yanik, A. A.; Altug, H.; Shvets, G. *Nat Mater* **2012**, *11*, 69.
- (2) Wiederrecht, G. P.; Wurtz, G. A.; Hranisavljevic, J. *Nano Letters* **2004**, *4*, 2121.
- (3) Yoshida, A.; Uchida, N.; Kometani, N. *Langmuir* **2009**, *25*, 11802.
- (4) Achermann, M. *The Journal of Physical Chemistry Letters* **2010**, *1*, 2837.
- (5) Fofang, N. T.; Grady, N. K.; Fan, Z.; Govorov, A. O.; Halas, N. J. *Nano Letters* **2011**, *11*, 1556.
- (6) Zengin, G.; Johansson, G.; Johansson, P.; Antosiewicz, T. J.; Käll, M.; Shegai, T. *Sci. Rep.* **2013**, *3*.
- (7) Murphy, C. J. *Anal. Chem.* **2002**, *74*, 520 A.
- (8) Govorov, A. O.; Carmeli, I. *Nano Letters* **2007**, *7*, 620.
- (9) Artuso, R. D.; Bryant, G. W. *Nano Letters* **2008**, *8*, 2106.
- (10) DeLacy, B. G.; Qiu, W.; Soljačić, M.; Hsu, C. W.; Miller, O. D.; Johnson, S. G.; Joannopoulos, J. D. *Optics Express* **2013**, *21*, 19103.
- (11) DeLacy, B. G.; Miller, O. D.; Hsu, C. W.; Zander, Z.; Lacey, S.; Yagloski, R.; Fountain, A. W.; Valdes, E.; Anquillare, E.; Soljačić, M.; Johnson, S. G.; Joannopoulos, J. D. *Nano Letters* **2015**, *15*, 2588.
- (12) Kometani, N.; Tsubonishi, M.; Fujita, T.; Asami, K.; Yonezawa, Y. *Langmuir* **2001**, *17*, 578.
- (13) Miroshnichenko, A. E.; Flach, S.; Kivshar, Y. S. *Reviews of Modern Physics* **2010**, *82*, 2257.
- (14) Satanin, A. M.; Joe, Y. S. *Physical Review B* **2005**, *71*, 205417.
- (15) Wu, X.; Gray, S. K.; Pelton, M. *Optics Express* **2010**, *18*, 23633.
- (16) Chen, H. L.; Gao, L. *Optics Express* **2013**, *21*, 23619.
- (17) Arruda, T. J.; Martinez, A. S.; Pinheiro, F. A. *Physical Review A* **2013**, *87*, 043841.
- (18) Gallinet, B.; Lovera, A.; Siegfried, T.; Sigg, H.; Martin, O. J. F. *AIP Conference Proceedings* **2012**, *1475*, 18.
- (19) Djoumessi Lekeufack, D.; Brioude, A.; Coleman, A. W.; Miele, P.; Bellessa, J.; De Zeng, L.; Stadelmann, P. *Applied Physics Letters* **2010**, *96*, 253107.
- (20) Schlather, A. E.; Large, N.; Urban, A. S.; Nordlander, P.; Halas, N. J. *Nano Letters* **2013**, *13*, 3281.
- (21) Melnikau, D.; Savateeva, D.; Susha, A.; Rogach, A.; Rakovich, Y. *Nanoscale Research Letters* **2013**, *8*, 134.
- (22) Gallinet, B.; Martin, O. J. F. *Physical Review B* **2011**, *83*, 235427.
- (23) In *Handbook of Optical Constants of Solids*; Palik, E. D., Ed.; Academic Press: Burlington, 1997.